Evaluation of indoor photovoltaic power production under directional and diffuse lighting conditions

Clément Antoine Reynaud, Raphaël Clerc, Pierre Balthazar Lechêne, Mathieu Hébert, Anthony Cazier, Ana Claudia Arias

Evaluation of indoor photovoltaic power production under directional and diffuse lighting conditions

Clément Reynaud[1†], Raphael Clerc[1], Pierre Balthazar Lechene[2], Mathieu Hebert[1], Anthony Cazier[1], Ana Claudia Arias[2].

1 Université de Lyon, UJM-Saint-Etienne, Institut d'Optique Graduate School, CNRS, UMR5516, Laboratoire Hubert Curien, F-42023, Saint-Etienne, France.
2 Department of Electrical Engineering and Computer Sciences, University of California, Berkeley, California 94720, USA
[†]corresponding author: clement.reynaud@im2np.fr

Abstract:

This work proposes a detailed method to estimate the amount of power produced by photovoltaic energy harvesting in realistic indoor conditions, not only featuring artificial light sources and low levels of irradiance (0.1 to 1 mW/cm²) but also oblique directional and diffuse lighting. The method is based on a model of performance of a commercial silicon and an organic solar cells under diffuse and oblique light and on simulations of indoor light in a rectangular room of various dimensions. It is found that the solar cells absorb diffuse light almost as efficiently as if it were direct normal light. Diffuse light accounts for 30 % to more than 70 % of the total illuminance in the indoor configurations investigated. Indoor, the angle of incidence at the point of maximum illuminance on a wall depends solely on the directivity of the source and is usually comprised within 30°-60°, representing 15 % to 50 % of power loss compared to normal incidence. The organic cell can achieve a power generation of up to 27 µW/cm² under 600 lux in a 4 m² room, and at least 7 µW/cm² under a typical indoor illuminance of 200 lux. The performance of the organic cell is found superior to the commercial silicon cell used in this study (7 µW/cm² under 600 lux), even if the power conversion efficiency of the silicon cell under one sun (12.7%) is higher than the one of the organic cell (5.4%).

Keywords: Energy harvesting, Photovoltaic, Indoor application, organic solar cells.

1. Introduction:

The emergence of the "Internet of Things" calls for the development of autonomous electronic devices [1]. Ideally, these devices should harvest energy from their environment, avoiding the need to be plugged in or the use of a battery that would need to be changed, especially for devices difficult to access [1][2]. Photovoltaic solar cells constitute a promising solution for such applications [1][2][3]. However, some use cases require the cells to operate indoors, where the lighting conditions differ significantly from those found outdoors for conventional photovoltaic installations. As a result, the standard methods to estimate the potential production of photovoltaic power cannot be used. In particular, the performance of a given cell in indoor conditions cannot be simply deduced from its outdoor characteristics. Indeed, solar cells are typically tested under optimistic outdoor conditions: solar spectrum of AM1.5, irradiance of 100 mW/cm^2, under normal incidence of light [4]. Indoor light differs from outdoor light in three considerable aspects: i) the light spectrum is different from the solar spectrum and depends on the nature of the source itself (Halogen, LED, CFL…), ii) irradiances are typically in the range of 0.1 - 1 mW/cm², much lower than 100 mW/cm^2, and iii) indoor light also rarely falls solely under direct normal incidence on the solar cells, but instead features both an oblique direct component and an isotropic diffuse component.

Only the first aspect (the impact of the artificial source spectrum) of this problem has been extensively discussed in the literature. Indeed, several work focus on the impact of lighting sources on several types of solar cells [5][6][7][8][9][11]. A major conclusion of these works is that the difference of power conversion efficiency (PCE) between silicon solar cells and their second and third generation competitors (amorphous silicon, CIGS, dye-sensitized and organic photovoltaic cells) is reduced when LED or CFL sources are considered instead of the sun itself, as they contain less radiative power in the infrared [9].

The second aspect (impact of the low level of irradiance on PCE) has been discussed in a limited number of recent papers [10][11][12][13][14]. In particular, organic photovoltaic (OPV) cells have

recently been reported to be among the most efficient for indoor use [11][12][13][14]. For instance, Lee *et al* have reported that an organic solar cell based on the donor polymer poly[N-9'-heptadecanyl-2,7-carbazole-alt-5,5-(4,7-di-2-thienyl-2',1',3'-ben-zothiadiazole)] (PCDTBT) could generate up to 13.9 μW/cm^2 of power under 300 lux from a CFL source, higher than other PV technology [11]. PCDTBT cells have also been demonstrated as successful energy harvester under indoor light when combined with super-capacitors [15] and have been shown to be very stable [16]. Finally, the fabrication process of OPV, compatible with high-throughput printing processes [17], allowing their easy production over large area, low cost and on flexible substrates, offers further advantages for indoor use. However, in all the previously mentioned papers, the solar cells efficiency has been measured under direct lighting at normal incidence, i.e. far from real indoor conditions.

Indeed, indoors, a solar cell receives both directional light from the source (typically under oblique incidence) and diffuse ambient light arising from multiple reflections on the walls and floor of the room, which results in a broad set of illuminations angles and often necessitates characterization in real rooms rather than on a test bench.

The impact of the light incidence angle has already been studied for solar cells and modules, but only in outdoor condition, for example by taking into account optical losses such as Fresnel reflectance to model the average power production over one year [15], or to enhance the performance of thin film organic solar cells [19][20][21]. Several procedures have been proposed to enhance the collection of grazing rays, by using textured films [22], photon trapping [23], photonic crystals [24], or nanoparticles [25]. Again in the case of outdoor use, one recent study [15] has concluded that improving light collection for high angles of incidence has little impact on the average power production over one year, as high incidence radiations are also penalized by an irradiance dimming proportional to the cosine of the incidence angle. Nonetheless, these conclusions are specific to outdoor conditions and cannot be transposed readily to the indoor case. Moreover, the light intensity and distribution in a room varies greatly with position, and where to place a solar cell to

maximize power production is not always straightforward, since directly under the light source is rarely practical.

The aim of this work is to evaluate the electrical power production of solar cells operating indoors, considering the influence of the directional and diffuse components of light, an issue, to the best our knowledge, which has never been addressed so far.

We show that the power production of a solar cell under oblique direct or diffuse light can be estimated from the characterization of its power production under normal direct incidence at various intensity. This estimation can be refined with an optical model of the angular dependence of light absorption by the solar cell. The procedure is validated experimentally with a commercial silicon solar cell and one our organic solar cell prototype. It is found that for both cells, the angular response is almost constant for incidence angles up to 60° (Si) and 70° (OPV). As a result, absorption of isotropic diffuse light is within 6 % as efficient as that of direct normal light. In order to determine the typical ranges of intensity and incidence angle distribution of indoor light, lighting simulations are performed for a rectangular room with varying dimensions and a single ceiling light source. The results suggest that diffuse light accounts for 30 % to 70 % of the total indoor illuminance, which falls between 600 lux and 100 lux. The position receiving the maximum illuminance on a wall can be predicted from the distance between the wall and the light source and from the source's directivity. At this position, the angle of incidence of direct light depends only on the directivity of the light source and is usually comprised between 30° and 60°. The combination of the room lighting model and of the solar cell absorption allows to predict the power production of the Si and OPV cells in typical indoor conditions. The OPV cell can achieve a power production above 20 µW/cm² under 600 lux of illuminance and about 10 µW/cm² under 200 lux in a 16 m^2 room. In the same conditions, the Si cell produces under 6 µW/cm² and about 1 µW/cm² respectively. Experimentally, the OPV cell produces up to 27 µW/cm² under a typical 4 000 lm LED ceiling source on the wall of a 7.21 m^2 real room, which is superior to the commercial silicon cell (up to 7 µW/cm^2), even if the PCE of the Si cell

under one sun (12.7%) is higher than the one of the organic cell (5.4%). These experimental values are close to the ones predicted by the model.

2. Materials and methods

2.1 Terminology

An important distinction has to be made between the terms irradiance and illuminance. Irradiance (W/m^2) is a power per unit area and is the unit used to measure the incoming power on PV devices. However, for indoor lighting, the figure of merit is the illuminance which measures the luminous flux per unit area. To be consistent with both the terms of the photovoltaic and indoor lighting community, we will use irradiance only when the characterization or modeling is independent of indoor or outdoor conditions. When simulating of measuring solar cells' efficiency in a room, we will use illuminance units.

2.2 Solar cell fabrication and characterization

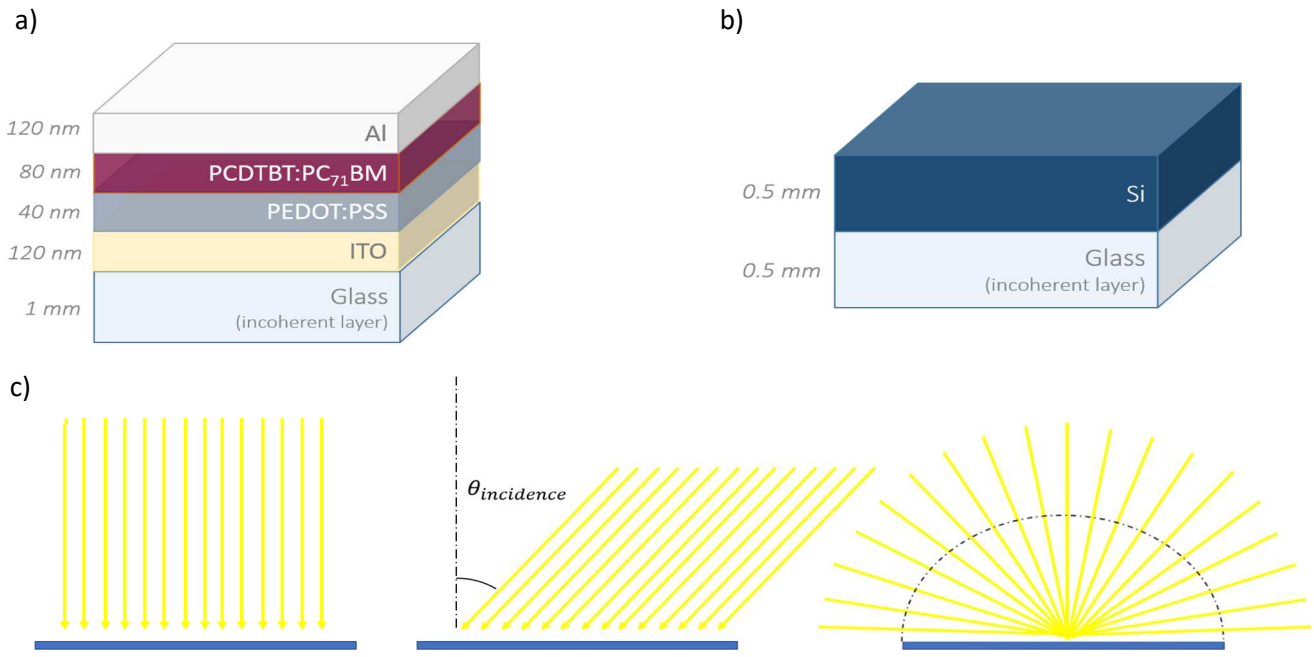

Figure 1 – a) structure of the organic solar cell used in this work b) simplified structure of the silicon solar cell used for the simulations. c) Schematics showing direct light hitting a substrate at direct normal incidence (left) or direct oblique incidence (middle), or diffuse light (right)

The silicon solar cell used in this study is a monocrystalline cell from Conrad Electronic featuring an area of 3.75 cm^2.

The organic solar cells were fabricated according to the structure described in figure 1a, following a procedure described in details in [11]: ITO-covered glass (from Thin Film Devices) were sequentially cleaned in acetone, isopropanol and water, then passed under UV-ozone plasma treatment for 30 min. PEDOT:PSS (Heraeus Clevios VPAI 4083, 40 nm) was spin-coated and baked at 180°C for 10 minutes. After transfer in a glovebox, a PCDTBT:$PC_{71}BM$ (1:4 in ortho-dichlorobenzene with 5% dimethyl sulfoxide) solution was spin-coated on top (80 nm). PCDTBT was purchased from Saint-Jean Photochimie and $PC_{71}BM$ from Solaris. Finally, polyethylenimine ethoxylated (PEIE, from Sigma Aldrich) diluted to 0.048 wt% in ethanol was also spin-coated and the whole device was annealed at 70°C for 10 minutes. 200 nm of aluminum were thermally evaporated to complete the devices, with an active area of 0.475 cm^2. The organic cells were specifically optimized to achieve good performance under low irradiance values, which in particular consists in minimizing the dark current of the cells [11]. The corresponding dark current was found in the order of $10^{-6} A/cm^2$ at -0.5V.

The solar cells' J-V curves were acquired using a Keithley 2400. The PCE [4] of both solar cells were measured at normal incidence, using both a solar simulator (from Newport Oriel Sol1A (xenon lamp)) and a 4000 lm LED luminaire (Philips LED PSED DN570B lamp). Both cells were tested under irradiances ranging from 0.01 mW/cm^2 up to 100 mW/cm^2, using neutral density filters from Newport and shadow masks. For the angular dependence of the short-circuit current, a halogen lamp with collimated beam and an irradiance of 1.1 mW/cm^2 was used.

2.3 Solar cell absorbance

The optical absorption of solar cells was estimated by modelling the propagation of light in each layer of the structure of the cell, as in ref [26]. Interference effects were taken into account in thin layers, and neglected for thick ones (> 300 µm), such as the 1mm glass substrate of the OPV cell [26][27]. Light scattering within the cell was also neglected. The wavelength-dependent real n and complex k optical index were extracted from spectral reflectance and transmittance measurements performed

on each layer, as indicated by Poelman *et al* [28]. For the commercial silicon cell, as the detailed structure of the cell is not known, the absorbance was calculated for a stack consisting of one layer of glass and one thick layer of silicon, neglecting the impact of any other layers as shown in figure 1b. The silicon spectral optical index (n,k) values were taken from ref [29].

2.4 Room lighting simulations

Simulations of the light illuminance distribution in a room were performed using the lighting design software Dialux [31]. In this software, the photometric characteristics of each source are imported from manufacturers, and the calculation of illuminance distribution is based on a radiosity model, which accounts for multiple light scattering by surfaces, assumed to be Lambertian (with a given albedo). In absence of specular surface, shadowing or natural daylight, the results of this type of software has been proven to be sufficiently accurate (~ 10% error on the values reported) to be used for quantitative studies [32]. The source used in this study was a 4000 lm LED luminaire (Philips LED PSED DN570B lamp), located on the ceiling at the center of the room and pointing directly down (see Fig. 3). In the simulation, the albedo of the room surfaces were taken equal to 0.5 for the floor and 0.7 for the ceiling and the walls, which corresponds to a realistic clear painted office with white dropped ceiling, white walls and parquet or linoleum floor.

3. Results and Discussion

3.1 Modeling the electrical power produced by a solar cell under oblique incidence and diffuse lighting.

Solar cells operating indoors receive light power from various angles of incidence, either as direct oblique light or as diffuse isotropic light (figure1 c). The light angle of incidence on a solar cells modify its production of electrical power in two ways: i) for a given light intensity, the incoming irradiance on a point of the cell's surface varies with the angle of incidence. In the case of a uniform parallel source, the power received from a ray at a given angle of incidence θ decreases by a factor cosθ compared to the normal incidence ii) not all incoming photons are absorbed by the photo-active layer of the solar cell because of optical losses such as Fresnel reflections at each interface within the cell, and parasitic absorption by other layers. Usually, the performance of solar cells are only measured and reported under direct normal incidence. Therefore, modeling the electrical power that a solar cell can produce in indoor conditions requires a method to determine the cell's power production under oblique and diffuse light from their standard characteristics under direct normal light.

Let us assume that a solar cell's power generation is known for each irradiance *E* under direct normal incidence $P_{0°}(E)$. The power production *P* of this solar cell under direct oblique light of irradiance E_θ (with θ the incidence angle) and under diffuse light of irradiance E_D can be calculated from $P_{0°}$ by calculating the effective irradiances E_θ^{eff} and E_D^{eff}, that would result in the same power production as the irradiances E_θ and E_D if they were hitting the cell at direct normal incidence:

$$\mathrm{P}(E_\theta + E_D) = \mathrm{P}_{0°}(E_\theta^{eff} + E_D^{eff}) \quad (1)$$

For oblique direct light, the effective irradiance E_θ^{eff} can be obtained from E_θ by :

$$E_\theta^{eff} = \frac{A(\theta)}{A(0)}\, E_\theta = \frac{A(\theta)}{A(0)} E_0\, cos\theta \quad (2)$$

Where A(θ) is the absorbance of the active layer of the solar cell under the incident angle θ and E_0 is the irradiance of the light received in direct normal conditions.

To determine E_D^{eff} from E_D, the diffuse light is considered under the Lambertian approximation where radiance is isotropic [30]. The irradiance dE received on an elementary surface by a ray of light contained in an elementary solid angle dΩ in a given direction making an angle θ with the normal of the surface is:

$$\mathrm{dE}(\theta, \varphi) = \mathrm{L}(\theta, \varphi)\cos(\theta)\,\mathrm{d}\Omega \tag{3}$$

Where L is the radiance and (θ,φ) spherical coordinates. In consequence, the total amount of diffuse irradiance E_D at a given point on a surface is obtained by integrating over every solid angle:

$$E_D = L\int_0^{2\pi} d\varphi \int_0^{\pi} cos\theta sin\theta d\theta = \pi L \tag{4}$$

The effective received diffuse irradiance E_D^{eff} is obtained from E_D by taking into account the angle dependent optical losses:

$$E_D^{eff} = L\int_0^{2\pi} d\varphi \int_0^{\pi} \frac{A(\theta)}{A(0)} cos\theta\ sin\theta\ d\theta = \beta\, E_D \tag{5}$$

with:

$$\beta = 2\int_0^{\pi} \frac{A(\theta)}{A(0)} cos\theta\ sin\theta\ d\theta \tag{6}$$

As a result, equation (1) can be re-written as:

$$\mathrm{P}(E_\theta + E_D) = \mathrm{P}_{0^\circ}\left(\frac{A(\theta)}{A(0)}E_\theta + \beta E_D\right) \tag{7}$$

Therefore, an estimation of $\frac{A(\theta)}{A(0)}$, the ratio of angular light absorption to normal light absorption of the solar cell's active layer is needed in order to relate *P* to P_{0°. To determine the angular absorption *A(θ)* of the two solar cells considered in this work, optical simulations based on a transfer matrix method (TMM) are performed [26]. Figure 2a shows *A(θ)*, as well as the reflectance *R(θ),* of the Si and OPV cells as a function of θ. These simulations are performed with an AM1.5 solar spectrum, but

no significant differences were observed when compared to a LED spectrum. No light is transmitted through the cells, and in the case of the OPV cell, the non-active layers contribute to parasitic absorption while the aluminum back contact ensure the total absorption of the remaining light. For both cells, the absorbance of the active layer is mostly constant, at 75 % for the silicon cell and 65% for the OPV cell until an incident angle of 70° after which it drops sharply. For the organic cell, there is even a slight rise between from 0° to 70°, with a maximum absorbance of 69%. From these simulations, the angular absorption ratio $\frac{A(\theta)}{A(0)}$, shown in Figure 2b, and the factor β can be calculated. The ratio $\frac{A(\theta)}{A(0)}$ is comprised between 0.95 and 1.05 for angles up to 58° and 68° for the Si and OPV cells respectively, suggesting that within these angular ranges, absorption of the active layer is almost identical to that at normal incidence. The factor β is found equal to 0.94 for the commercial silicon cell and 0.98 for the organic cell. These values are close to 1, indicating that both solar cells convert diffuse light into electrical power almost as efficiently as if the same irradiance was seen under normal incidence. This is due to the weak angle dependence of the absorbance A(θ) for low incidence angle (θ < 60°), which contains most of the irradiance in the case of Lambertian diffuse lighting.

In order to validate the optical simulations, their results are compared to experimental

measurements of the angular variation of the short-circuit currents of the two photovoltaic cells,

since the short-circuit current is directly proportional to light absorption in the active layer. Figure 2c

shows the experimental results, along with the cosθ baseline variation of the irradiance and the

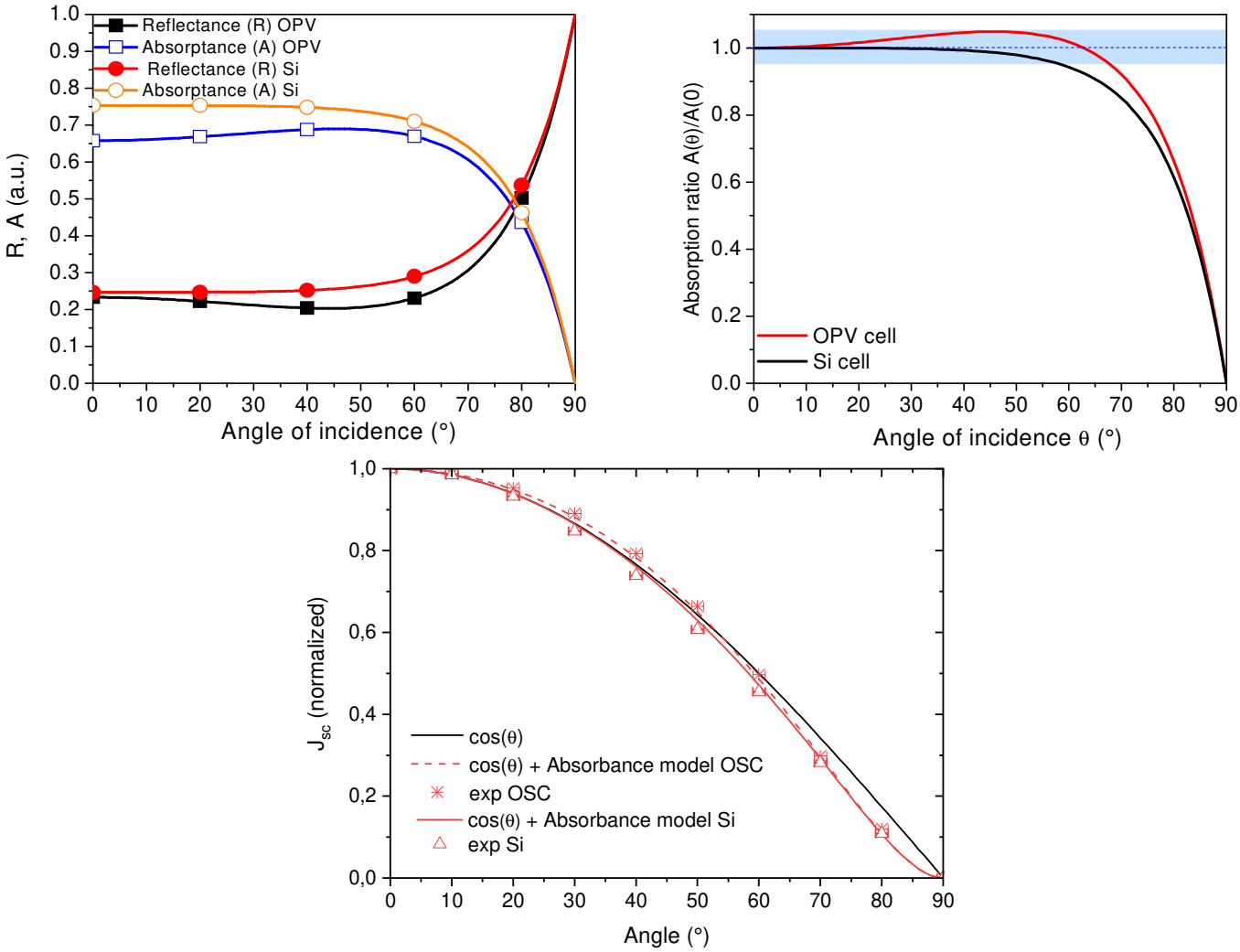

Figure 2 - a) Simulation of the Absorbance of the active layer (open symbols) and Reflectance (full symbols) of the organic solar cell (squares) and silicon solar cell (circles) as a function of the light angle of incidence. c) Absorption ratio (ϑ)/(0) as a function of the angle of indicence ϑ for the two solar cells. c) Normalized short circuit current as a function of the light angle of incidence ϑ for the two solar cells as given by experimental values or the simulation model. The values of cos(ϑ) are also shown as a reference

a) b)

simulation results referred as "absorbance model". The simulation is found to reproduce the

c)

experimental data the most accurately for both solar cells. In particular for the OPV cell, the model is able to successfully predict the higher experimental short-circuit current than the theoretical cosθ decay for angles between 10 and 50 degrees because of the higher value of $\frac{A(\theta)}{A(0)}$ at these angles. Such a behavior is not visible for the silicon solar cell. These results confirm that the optical simulation accurately describes the angular absorption of the two solar cells. Thus, by inserting within equation 7 the output of this model and the normal incidence power output of a given solar cell, it is possible to predict the power this cell would produce under any scenario of light incidence. Moreover, the findings that $\frac{A(\theta)}{A(0)}$ is within 5% of unity for angles up to 60° and that β is also close to 1 for both cells suggest that by using default values for these parameters into equation 7 could allow to estimate the indoor production potential of any solar cell. Equation 7 which relates P to P_0 is based on two assumptions: i) that the short circuit current of the cell is directly proportional to the absorbance, and ii) that the solar cell's fill factor and open circuit voltage are not impacted by the variation of absorbed light power. This can be expected to be generally true for angles of incidence between 0 and 80 degrees, since the overall light absorbed has a similar order of magnitude (Figure 2. B). However, above 80 degrees of direct light incidence, the actual power produced by the cell may vary because of variation of fill factor and open circuit voltage.

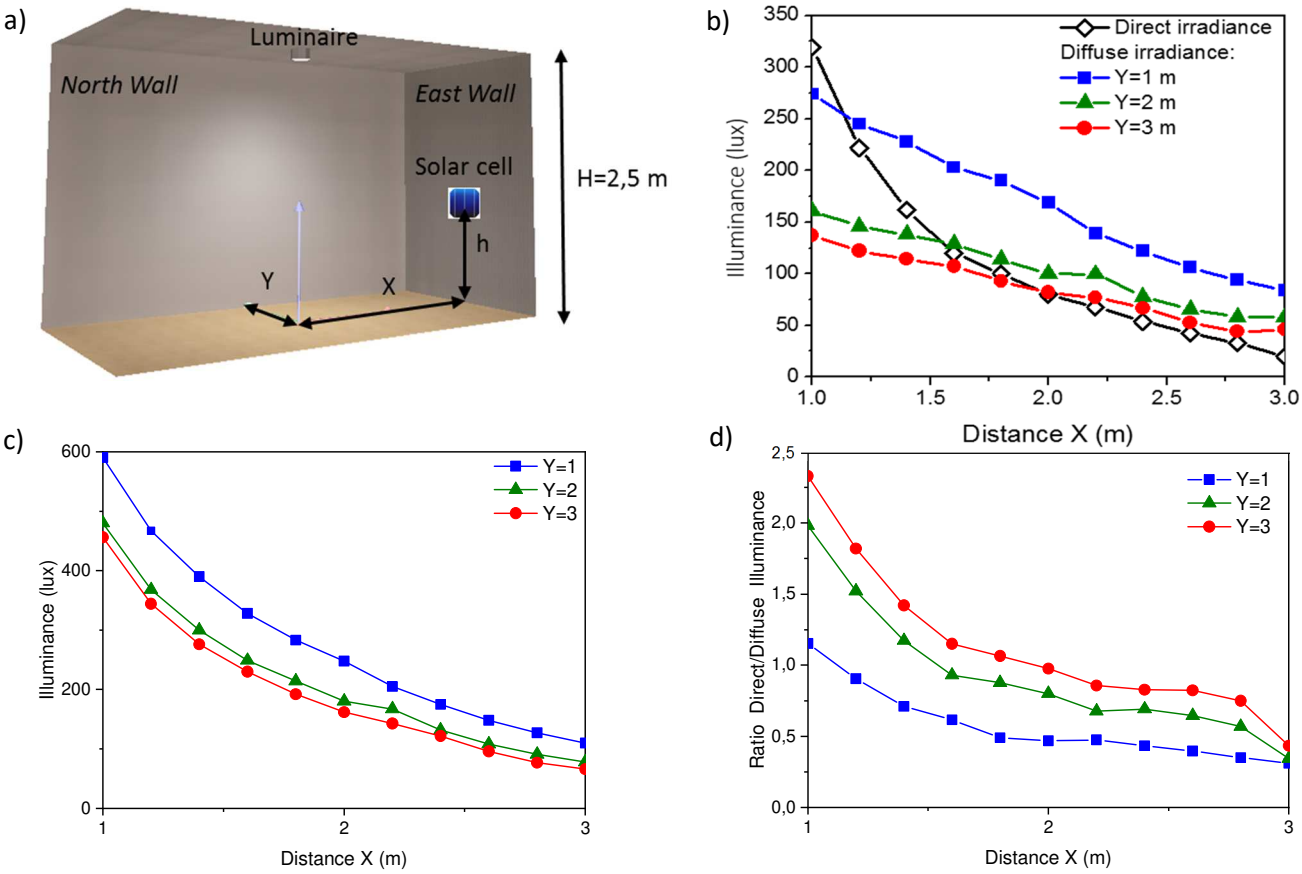

Figure 3 – a) schematic of the rectangular room simulated. b) Direct and diffuse illuminance and c) Total illuminancereceived by the East wall at the point of maximum illuminance as a function of the room dimensions X and Y. d) Ratio of the direct over diffuse illuminance at the point of maximum illuminance on the East wall as a function of the X and Y dimensions.

3.2 Evaluation of typical diffuse and direct illuminance in a rectangular room.

The power and composition of light available in a room depends strongly on the geometry of the room, the type and placement of light sources, the nature of the room's surfaces, and the position considered within the room. In order to estimate the power production potential of a PV cell operating indoors using equation 7, the typical real-life ranges of value for E_θ and E_D must be identified. To do so, quantitative lighting simulations are performed using the commercial software Dialux, for an idealized closed rectangular room. The room, shown in Figure 3a, has a single 4000 lm LED light source in the center of the ceiling, no window, and a constant ceiling height *H* = 2.5 m. The *X*-*Y* dimensions are varied from *X* = *Y* = 1m (a small 4 m^2 room like a closet) to *X* = *Y* = 3 m (a 36 m^2 room). Larger rooms are not considered since they would realistically be equipped with more than one light source. The luminaire was chosen so that the illuminance in the center of the room directly

underneath ranges between 500 lux and 700 lux for all room sizes. On the floor in the center of the room, the light intensity for X=Y=1m is 660 lux, with a light composed at 55% of direct and 45% of diffuse ($\frac{E_D}{E_\theta}$ =1.2). For X=Y=3m, the center floor light intensity is 520 lux, with $\frac{E_D}{E_\theta}$ = 2.5 (diffuse light accounts for 29 % of the total illuminance). At the point of maximum total illuminance on the East wall, the direct E_D and diffuse E_θ values of illuminance are investigated: Figure 3b shows their evolution as a function of the room's dimensions (the direct illuminance is unaffected by changes in Y), and figure 3c shows the total maximum illuminance received on the wall. Figure 3c shows the direct/diffuse ratio $\frac{E_D}{E_\theta}$ as a function of the room dimensions. The highest illuminances on the wall, 450-600 lux, are obtained for X=1 m and decrease with increasing X values until 66-110 lux. The variations of illuminance between Y=1m and Y=3m range between 20 % (X=1m) and 40% (X=3m). The distance of the East wall from the light source is the strongest factor of influence of the illuminance received by the wall. For the direct/diffuse ratio, the highest values are obtained with smaller values of X and decrease as X increase: the range of $\frac{E_D}{E_\theta}$ starts from 1.2-2.4 for X=1 m (Y between 1 and 3m) and decreases to 0.2-0.6 for X=3m. In this last case, diffuse light accounts for 83% to 62% of the total illuminance. The Y dimension greatly influences the ratio of $\frac{E_D}{E_\theta}$: for X=1m, the ratio goes from 2.3 for Y=3m to 1.1 for Y=1m. This shows that the light reflected by the North-South walls contributes significantly to diffuse light and to the total illuminance received by the East wall. In general, diffuse light is significant for the light intensity, since $\frac{E_D}{E_\theta}$ is always below 2.5 even for the largest room, meaning diffuse light accounts for at least one third of the total intensity in any situation. Diffuse light even becomes dominant for rooms with X>2 m. In a typical indoor room, the average ambient illuminance should be at least 200-500 lux for comfortable human vision, so the results suggest that rooms with X larger than 2.5 m would likely be equipped with more than one source in a realistic setting.

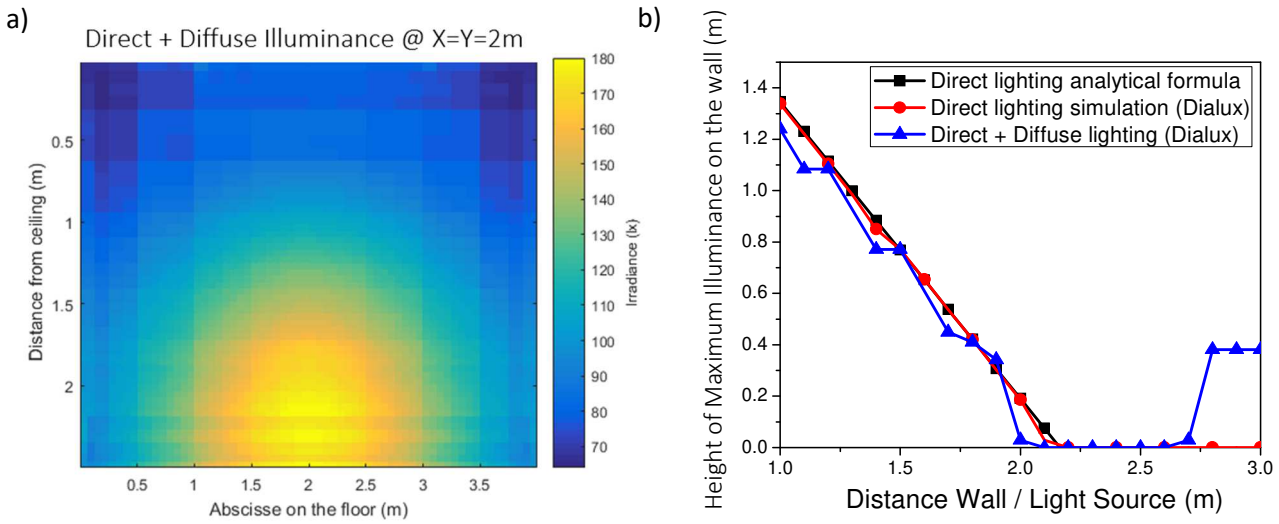

Figure 4 – a) Map of the East wall showing the total illuminance received as a function of the position on the wall. b) Vertical position of the point of maximum illuminance on a wall as a function of the distance between the wall and the ceiling light source (X), computed either from the theoretical model (black squares), from the lighting simulation taking only the direct light component (red circles), and from the complete lighting simulation (blue triangles).

Ideally, solar cells should be positioned in the place receiving the highest illuminance on a wall, and the angle of incidence of direct light in this position must be known in order to predict the cell's power production. Within a given room, the light intensity varies greatly with the position considered on the wall. As an example, figure 4a shows the distribution of illuminance on the East wall as a function of position on the wall for a room with X=Y=2m. The light illuminance varies three-fold depending on the point considered on the wall: from 180 lux at the brightest to 60 lux in the darkest corners. There is a large bright spot in the zone where light from the source hits the wall directly. The shape and spread of the bright spot depends on the source's characteristics. Because the room is symmetrical, the position of maximum illuminance is always situated in the middle of the horizontal axis. The vertical position of this maximum depends on the dimensions of the room. For direct light coming from the light source, it can be demonstrated (see Appendix A) that h_{opt}, the height of the maximum of illuminance is:

$$h_{opt} = H - \frac{X\sqrt{3m}}{3} \qquad (8)$$

Where H is the ceiling height and m is a parameter that quantify the the source directivity following $I(\theta) = I_0 \cos^m(\theta)$. m = 1 corresponds to the case of lambertian source, and m >> 1 to a highly directional source. . For the lamp considered, m=4. Figure 4b gives the height of maximum

illuminance on the wall as a function of the room's X dimension for the direct light as calculated from equation 8, for the direct light obtained from the DIALUX simulations and for the total of direct and diffuse light from the simulations. The analytical model and simulations are in excellent agreement for the direct light. For the total illuminance, comprising direct and diffuse light, the position of the maximum is slightly lower than that of direct light alone. This is due to the fact that diffuse illuminance is slightly higher near the ground because of the reflections coming from the floor. The step-like behavior of the graph is due to the mesh approximations used by DIALUX. Overall, the maximum of illuminance is situated in the middle of the wall for X=1 and slides down as X increases, until X=2.2m. Passed this value, the light does not hit the wall directly and the illuminance on the wall is only composed of diffuse light. Similarly to equation 8, the angle of incidence α_{opt} at which the direct light hits the wall at the position of maximum illuminance can be analytically calculated:

$$\cos \alpha_{opt} = \frac{1}{(1 + m/3)^{1/2}} \tag{9}$$

The angle of incidence depends only on the lamp's directivity. For a Lambertian source (*m=1*), α_{opt} = 30° and α_{opt} increases with m, i.e. as the source becomes more and more directive. For the source used here, m=4 and α_{opt} = 49°. In conclusion, the ideal position for a solar cell on a wall is at the point of maximum illuminance, which depends on the wall's distance to the light source, and on the directivity of the source. At this position, the angle of incidence of the light depends solely on the directivity of the light source. The distance of the perpendicular walls to the source also affects the amount of diffuse light received by the solar cell.

3.3 Prediction of the power produced by a photovoltaic cell operating indoor.

3.3.1 Power produced in a rectangular room

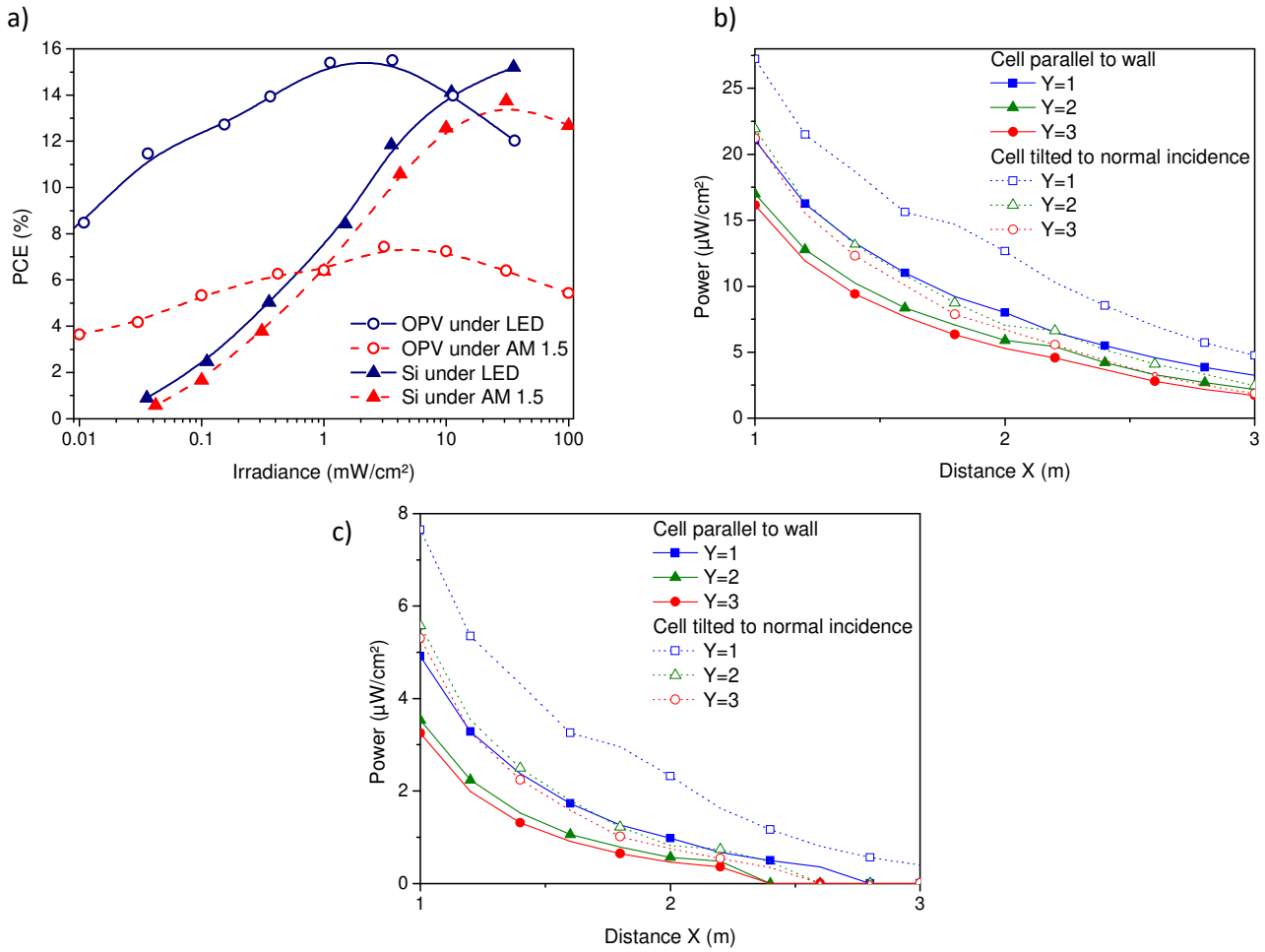

Figure 5 – a) Power conversion efficiency of the Silicon solar cell (triangle) and organic solar cell (stars) as a function of light intensity from an LED source (blue) or the standard sun AM1.5 spectrum (red). The lines represent fits used to interpolate the experimental data. b) and b) Simulation of the power generated under LED illumination by the organic solar cell and silicon solar cell respectively as a function of the room dimensions in the case where they are flat on the wall (full symbols) or tilted to receive direct light at normal incidence (open symbols).

The combination of the model of solar cell's power generation (equation 7) with the simulations of indoor illuminance allows to evaluate the range of electrical power a solar cell could produce in a typical room. Figure 5A shows the PCE of the Si and OPV cells as a function of light intensity for two light sources: the standard sun AM1.5 spectrum and the LED light used in the simulations. Under the sun spectrum and in the range of high irradiance (1-100 mW/cm^2), the Si solar cell has a maximum PCE of 13.7%, largely outperforming the OPV cell which has a maximum PCE of 7.4% in these conditions. However, in the low light range (0.01-1 mW/cm^2), the PCE of the Si cell decreases sharply and falls below 1.5 % at 0.1 mW/cm^2 of intensity. At this intensity, the PCE of the OPV cell hovers at 5.3% and is still above 3.7 % at the lowest Intensity. Under the LED light, the Si cell performs similarly to under the sun spectrum. Meanwhile, the PCE of the OPV cell is far greater under the LED light: it has a maximum of 15.5% at 10 mW/cm^2 and remains above 10 % until 0.05 mW/cm^2. Indoor light usually falls in the range of 200-500 lux, which corresponds to an intensity of 0.18-0.45 mW/cm^2 for sun light and an intensity of 0.06-0.15 mW/cm^2 for the LED light. Using equation 7 with these characterizations, the calculation of $\frac{A(\theta)}{A(0)}$ and the room light simulations allows to calculate the amount of electrical power generated by the solar cells as if they were situated at the point of maximum light illuminance in rectangular rooms of varying dimensions. The results are given in figure 5b and 5c for the OPV and Si cells respectively, in two configurations: if the cells are placed flat on the wall or if they are tilted to receive normal incidence from the light source. As suggested by the PCE measurements, the power generated by the OPV cell surpasses that of the Si cell. For rooms with X=1m and Y between 1 and 3m the OPV cell generates between 16 and 22 µW/cm^2 of electrical power if flat on the wall, and up to 27 µW/cm^2 if tilted to normal illuminance. In these conditions, the Si cell generates 3.5 to 5.5 µW/cm^2 if flat and up to 8 µW/cm^2 when tilted. When the dimensions of the room increase, the power generated decreases along with the amount of light illuminance. For X=3m, the illuminance is between 66 and 110 lux and the OPV cell only generates 1.7 to 3 µW/cm^2

(flat) and at most 4.8 μW/cm^2 if tilted. The Si cell power production falls to 0 μW/cm^2 around X=2.5m. When the cells are tilted to receive direct light under normal incidence, the power generated is higher than when they are flat on the wall, due to the reduction of optical losses for the direct light. This is particularly marked when the total illuminance is composed principally from direct light: when X=1m, the case where direct light is the most predominant (see figures 3b and 3d), cells with normal incidence orientation can generate up to 30% more power than if they are flat on the wall. When X increases, the light is composed of more diffuse light and the difference of power generated between the two cell orientations decreases. In most typical indoor settings, the maximum of illuminance is required to be at least 200 lux, in which conditions, the OPV cell produces approximately 7 μW/cm^2 and the Si cell under 1 μW/cm^2. These results show that the OPV cell can generate significantly more power in indoor conditions than the Si cell. Since the efficiency of OPV under low sunlight irradiance is higher than that of the Si cell, this conclusion would likely remain true even in more varied indoor settings, such as cases where a window provides partial sunlight into the room.

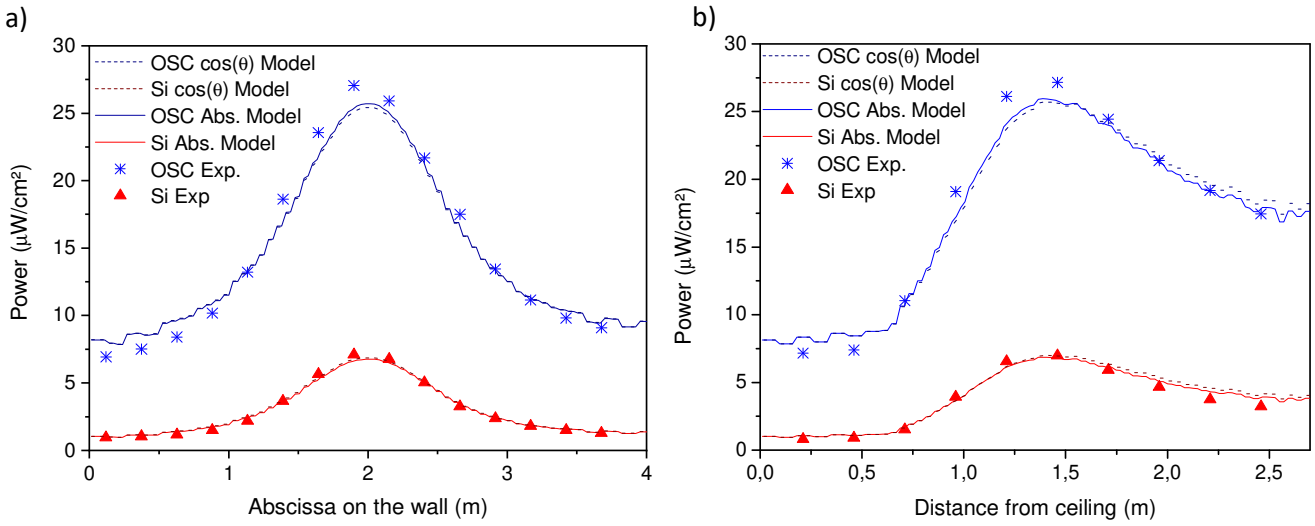

Figure 6 - Power generated by the silicon solar cell (red) and organic solar cell (blue) as a function of their position on a wall, either at a fixed height of 1.5 m and varying horizontal position (a) or at the horizontal center and varying heights on the wall (b). The values are either obtained from experimental measures (discrete points) or simulations using either the cos(ϑ) model (dotted lines) or the cell absorption model (plain lines).

3.3.2 Experimental verification of the model

In order to validate the model of solar cell power generation, its results are compared with experiments performed in a real room. The room's dimensions are X = 0.89 m, Y = 2.025 m (7.21 m^2) and H = 2.71 m, and is equipped with the same commercial light source as in the simulations, placed in the middle of the ceiling. Simulations of the light composition and illuminance on one of the walls are performed with DIALUX. The power produced by the two solar cells at different positions flat on the wall is predicted using the characterization of Figure 5A and equation 7, with the values of $\frac{A(\theta)}{A(0)}$ either taken from the simulated absorption or simply equal to cos(θ). Measurements of the power generated by the solar cells at different points on the wall are performed. Figures 6a and 6b show the power produced by the solar cells experimentally and according to the two simulations at a fixed height of 1.5m for different horizontal positions on the wall (6a) and at the horizontal center of the wall for different heights respectively (6b). Experimentally, the maximum power generated is 7 µW/cm^2 for the Si cell and 27 µW/cm^2 for the OPV cell, which confirms the potential of organic solar cells to serve as indoor energy harvesters. The generated power predicted from the simulation using

the modeled value of $\frac{A(\theta)}{A(0)}$ is closer to the experimental results than the simulation using only cos(θ), but the difference between the two is very small (at most 2%), indicating that the cos(θ) approximation is valid for practical uses. The mean error between the simulations using $\frac{A(\theta)}{A(0)}$ and the experimental values is 7% for the organic solar cell and 10.7% for the Si cell. Overall, the simulations and the experiments are in good agreement for all positions on the wall, which confirms the validity of the model.

4 Conclusion:

In summary, the method developed combines the characterization of solar cells under normal direct light, a model of their effective absorption under varying incidence angles, and simulations of illuminance levels within a room. It can accurately predict a cell's power production in indoor conditions and could guide the development of best practices on how to design, position, and use solar cells indoors. In particular, the results highlight the importance of indoor diffuse light, which corresponds to at least 30 % and up to 70 % of the total illuminance, and is absorbed by solar cells almost as efficiently as if it was received under direct normal incidence. Under indoor light, the OPV cell produces significantly and consistently more power than the Si cell, even though the PCE of the Si cell under 1-sun (12.7%) is much better than the organic cell's (5.4%). The OPV cell generates up to 27 μW/cm^2 under 600 lux of LED light, and at least 7 μW/cm^2 under 200 lux, the typical lower bound of illuminance in practical indoor settings. These levels of electrical power production are encouraging for the application of solar cells, and especially organic solar cells, as a source of energy for indoor autonomous devices.

Acknowledgments :

This work was partially supported by the National Science Foundation under Grant No 1610899 and by the France Berkeley Fund FBF #2015---03.

The authors would like to thank Gregory Duchene (PISEO) for helpful discussions.

References :

[1] H. Sundmaeker, P. Guillemin, P. Friess, S. Woelfflé, S. "Vision and challenges for realising the Internet of Things". *Cluster of European Research Projects on the Internet of Things, European Commision*. Luxembourg: Publications Office of the European Union (2010).

[2] L. Mateu, F. Moll, "Review of energy harvesting techniques and applications for microelectronics" in Microtechnologies for the New Millennium 2005 (pp. 359-373). International Society for Optics and Photonics (2005).

[3] A. Hande, T. Polk, W. Walker, D. Bhatia "Indoor solar energy harvesting for sensor network router nodes". Microprocessors and Microsystems, 31(6), 420-432 (2007).

[4] M. A. Green "Solar cells: operating principles, technology, and system applications" Prentice-Hall, Inc.,Englewood Cliffs, NJ (1982)

[5] B. Minnaert and P. Veelaert, "A proposal for typical artificial light sources for the characterization of indoor photovoltaic applications," *Energies*, vol. 7, no. 3, pp. 1500–1516, 2014.

[6] K. Cnops, E. Voroshazi, C. Hart De Ruijter, P. Heremans, and D. Cheyns, "Organic photovoltaic cell relying on energy transfer with over 20% efficiency in indoor lighting," *2014 IEEE 40th Photovolt. Spec. Conf. PVSC 2014*, pp. 143–146, 2014.

[7] A. Sacco, L. Rolle, L. Scaltrito, E. Tresso, C. F. Pirri. "Characterization of photovoltaic modules for low-power indoor application". Applied energy, 102, 1295-1302 (2013)

[8] F. De Rossi, T. Pontecorvo, T. M. Brown. "Characterization of photovoltaic devices for indoor light harvesting and customization of flexible dye solar cells to deliver superior efficiency under artificial lighting". Applied Energy, 156, 413-422. (2015)

[9] M. Freunek, M. Freunek, L. M. Reindl, "Maximum efficiencies of indoor photovoltaic devices" IEEE Journal of Photovoltaics, 2013, vol. 3, no 1, p. 59-64.

[10] J. Russo, W. Ray, M. S. Litz (2017) " Low light illumination study on commercially available homojunction photovoltaic cells" *Appl. Energy*, 191, 10.

[11] H. K. Lee, Z. Li, J. R. Durrant, W. C. Tsoi, (2016). "Is organic photovoltaics promising for indoor applications?". *Applied Physics Letters*, *108*(25), 253301.

[12] Y. Aoki (2017) "Photovoltaic performance of Organic Photovoltaics for indoor energy harvester" *Org. Electron* 48, 194.

[13] Harrison Ka Hin Lee et al, "Organic photovoltaic cells – promising indoor light harvesters for self-sustainable electronics" *J. Mater. Chem.* A 2018, 8.

[14] C. L. Cutting, M. Baga, D. Venkataraman (2016) "Indoor Light Recycling: A New Home for Organic Photovoltaics" *J. Mater. Chem. C*, 4, 10367.

[15] B. P. Lechêne, M. Cowell, A. Pierre, J. W. Evans, P. K. Wright, and A. C. Arias, "Organic solar cells and fully printed super-capacitors optimized for indoor light energy harvesting," *Nano Energy*, vol. 26, pp. 631–640, 2016.C.

[16] H. Peters et al. "High efficiency polymer solar cells with long operating lifetimes." Advanced Energy Materials 1.4 (2011): 491-494.

[17] H. Kang et al, "Bulk-Heterojunction Organic Solar Cells: Five Core Technologies for Their Commercialization". Adv. Mat.. DOI: 10.1002/adma.201601197 (2016)

[18] M. Ebert, H. Stascheit, I. Hädrich, and U. Eitner, “The Impact of Angular Dependent Loss Measurement on PV Module Energy Yield Prediction” *International Photovoltaic Science and Engineering Conference 29th*, vol. 49, no. September, 2014.

[19] D. Cheyns, B. P. Rand, B. Verreet, J. Genoe, J. Poortmans, and P. Heremans, “The angular response of ultrathin film organic solar cells,” *Appl. Phys. Lett.*, vol. 92, no. 24, pp. 1–4, 2008.

[20] S. Lee, I. Jeong, H. P. Kim, S. Y. Hwang, T. J. Kim, Y. D. Kim, J. Jang, and J. Kim, “Effect of incidence angle and polarization on the optimized layer structure of organic solar cells,” *Sol. Energy Mater. Sol. Cells*, vol. 118, pp. 9–17, 2013.

[21] Y. Lee, K. Kang, S. Lee, et al. "Integrated optoelectronic model for organic solar cells based on the finite element method including the effect of oblique sunlight incidence and a non-ohmic electrode contact" Japanese Journal of Applied Physics, 2016, vol. 55, no 10, p. 102301.

[22] J. B. Kim, P. Kim, N. C. Pégard, S. J. Oh, C. R. Kagan, J. W. Fleischer, H. a. Stone, and Y.-L. Loo, “Wrinkles and deep folds as photonic structures in photovoltaics,” *Nat. Photonics*, vol. 6, no. 5, pp. 327–332, 2012.

[23] S. J. Kim, G. Y. Margulis, S. Rim, M. L. Brongersma, M. D. Mcgehee, and P. Peumans, “Geometric light trapping with a V-trap for efficient organic solar cells,” vol. 21, no. May, pp. 572–576, 2013.

[24] L. Zeng, Y. Yi, C. Hong, J. Liu, N. Feng, X. Duan, L. C. Kimerling, and B. A. Alamariu, “Efficiency enhancement in Si solar cells by textured photonic crystal back reflector,” *Appl. Phys. Lett.*, vol. 89, no. 11, pp. 1–4, 2006.

[25] K. Nakayama, K. Tanabe, and H. A. Atwater, “Plasmonic nanoparticle enhanced light absorption in GaAs solar cells,” *Appl. Phys. Lett.*, vol. 93, no. 12, 2008.

[26] H. A. Macleod, "Thin-film optical filters" CRC press (2001)

[27] L. Simonot and S. Mazauric, “Matrix method to predict the spectral reflectance of stratified surfaces including thick layers and thin films Matrix method to predict the spectral reflectance of stratified surfaces including thick layers and thin films,” no. MAY, 2015.

[28] D. Poelman, P. F. Smet "Methods for the determination of the optical constants of thin films from single transmission measurements: a critical review". Journal of Physics D: Applied Physics, 36(15), 1850 (2003).

[29] M. A. Green, "Self-consistent optical parameters of intrinsic silicon at 300K including temperature coefficients". Solar Energy Materials and Solar Cells, 92(11), 1305-1310 (2008).

[30] J. L. Meyzonnette, T. Lépine "Bases de radiométrie optique" Cépaduès (2001).

[31] DIALux, Light Building Software, www.dial.com.

[32] C. E. Ochoa, M. B. C. Aries, and J. L. M. Hensen, “State of the art in lighting simulation for building science: a literature review,” *J. Build. Perform. Simul.*, vol. 5, no. 4, pp. 209–233, 2012.

[33] I. Moreno, M. Avendaño-Alejo, R. Tzonchev, "Designing light-emitting diode arrays for uniform near-field irradiance" Applied optics, 45(10), 2265-2272 (2006).